PHILOSOPHICAL TRANSACTIONS OF THE ROYAL SOCIETY B BIOLOGICAL SCIENCES

On the Relation Between Displacement Currents and Activation of the Sodium Conductance in the Squid Giant Axon

E. Rojas and R. D. Keynes

Phil. Trans. R. Soc. Lond. B 1975 **270**, 459-482
doi: 10.1098/rstb.1975.0023

Phil. Trans. R. Soc. Lond. B. **270**, 459–482 (1975) [459]
Printed in Great Britain

On the relation between displacement currents and activation of the sodium conductance in the squid giant axon

By E. Rojas† and R. D. Keynes, F.R.S.
Laboratory of the Marine Biological Association, Plymouth; Laboratorio de Fisiología Celular, Universidad de Chile, Chile; Physiological Laboratory, Cambridge

The early time course of the current passing across the membrane in squid giant axons in which the ionic currents have been blocked reveals substantial asymmetries during and after the application of hyperpolarizing and depolarizing voltage-clamp pulses of identical size. Since the integral of the 'on' and 'off' current transients is zero, these currents must result from charge movements confined to the membrane and, therefore, they are nonlinear displacement currents.

The steady state rearrangement of the charges as a consequence of sudden displacements of the membrane potential is consistent with a Boltzmann distribution of charges between two states characterized by different energy levels. Following changes in membrane potential the charges undergo a first order transition between these states. The relaxation time constant for the transition at a given temperature is a function of membrane potential. We propose that these displacement currents arise from a redistribution of the charges involved in the sodium gating system.

1. Introduction

The most distinct characteristics of the electrical activity of nerve membranes, as determined from voltage-clamp experiments, can be summarized as follows.

(*a*) There are two independent kinetic components in the membrane currents associated with a sudden decrease in membrane potential. Each component represents an ionic pathway with different ionic selectivity.

(*b*) The instantaneous currents through each pathway are linearly dependent on the membrane potential. These currents are characterized by driving forces appropriate to ions moving passively down an electrochemical gradient.

(*c*) The ionic conductances are activated by changes in the electric field across the membrane. The dependence of the sodium conductance upon potential gives rise to the apparent negative resistance region of the current–voltage relations for the sodium currents.

Most of these features can be concisely described in terms of the Hodgkin & Huxley equations (1952). Thus, ionic current records are accounted for by postulating the existence of three voltage-dependent first-order reactions. The fastest of these, described by the Hodgkin–Huxley variable m, controls the activation of the inward sodium currents. The slower reactions, h and n, control the inactivation of the sodium current and the activation of the outward potassium current respectively. Thus,

$$\mathrm{d}k/\mathrm{d}t = \alpha_k (1-k) - \beta_k k, \tag{1}$$

where $k = m$, h or n, and α_k and β_k are rate coefficients, which are functions of the electrical potential across the membrane.

† Present address: Laboratoire de Neurobiologie, École Normale Supérieure, 46 Rue d'Ulm, 75230 Paris Cédex 05.

The simplest interpretation of these variables is that they describe distinct 'gating processes' which depend fundamentally on the effects of the electric field on the distribution or orientation of membrane molecules with a charge or dipole moment, and which operate in association with the individual sodium and potassium channels. When, therefore, the membrane potential is suddenly decreased, the passage of each ionic current must be preceded not only by the surge of capacity current, but also by what has come to be known as the 'gating current', produced by the movement of these charges within the membrane (Armstrong & Bezanilla 1974; Keynes & Rojas 1974).

The main difficulty in proposing a definite experimental test for this hypothesis has been the lack of a method to measure directly the voltage dependent molecular rearrangement in excitable membranes. During the summer of 1971 one of us (E.R.), working at the Marine Biological Laboratory, Woods Hole, together with F. Bezanilla, used averaging techniques to observe, for the first time, asymmetrical currents during and after the application of hyperpolarizing and depolarizing pulses of identical size across the membrane of a squid nerve fibre in which the ionic currents had been blocked.

We present now experimental evidence which demonstrates that these asymmetrical currents are displacement currents, i.e. they are originated by the movement of charges confined to the membrane. In the absence of a more detailed knowledge of the chemistry of the axolemma, and due to the lack of specificity of the electrical measurements employed, it is impossible to propose a specific molecular model. However, we see no formal differences between the mathematical description of the Hodgkin–Huxley m and h gating processes and that used in the present work to account for the kinetic and steady state properties of the observed displacement currents. Although the evidence presented here is far from being conclusive, it suggests that, as a consequence of sudden displacements of the membrane potential, membrane charges undergo a rearrangement which is a first order transition between two states characterized by different energy levels. Furthermore, the energy difference between these two states is a linear function of the electrical potential across the membrane. The evidence is also consistent with the proposition that the energy difference between each state and the energy barrier for the transition is again a linear function of the field across the membrane.

An extensive account of the experimental methods employed here, and of some of the results, has been published elsewhere (Keynes & Rojas 1974).

2. Early symmetrical displacement currents

Our studies of the dielectric properties of the axolemma of a giant nerve fibre suggest that the total membrane capacitance is made up of two components. One of them is independent of the electrical potential difference across the membrane and, therefore, exhibits a linear behaviour during sudden displacements of the membrane potential. On the other hand, displacement currents through the second of these two components exhibit nonlinear characteristics. To determine accurately the characteristics of the displacement currents, it is necessary first to eliminate the ionic currents, which are much larger and obviously nonlinear. In the present experiments this was achieved by various ionic substitutions of permeant ions by impermeant ones, and by using tetrodotoxin (TTX) to block the selectivity filter of the sodium system.

Figure 1 shows two current transients obtained under voltage clamp conditions. The

membrane potential was suddenly displaced from -80 to $+20$ mV (absolute membrane potentials are referred to the external solution as ground; positive going changes are referred to as depolarizations and negative going ones as hyperpolarizations) giving rise to the outward current transient seen in this figure. The inward current transient for the hyperpolarizing displacement of the membrane potential from -80 to -180 mV, also shown in this figure, is almost identical to the outward current transient.

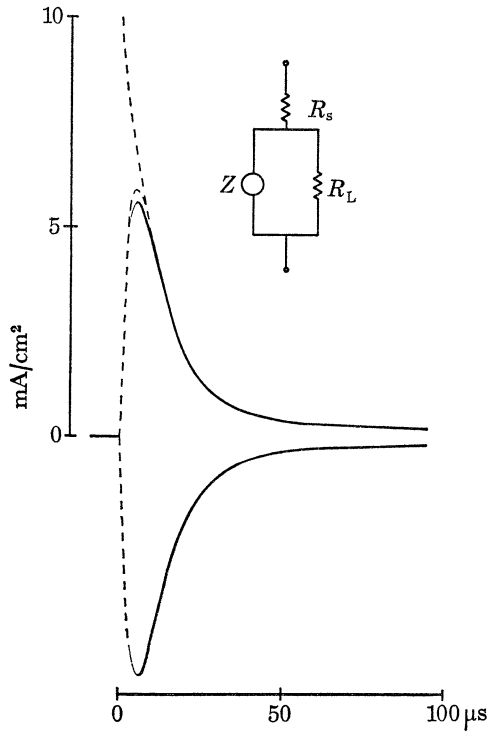

FIGURE 1. Capacitative current transients under voltage-clamp conditions. Fibre internally perfused with 300 mM CsF, 600 mM sucrose, 5 mM tris Cl, pH = 7.3, and immersed in a Na- and K-free saline with tetrodotoxin (440 mM tris Cl, 10 mM $CaCl_2$, 50 mM $MgCl_2$, 300 mM TTX, pH = 7.3). Series resistance compensation for 2.0 Ω cm². Temperature of the external solution was 7.8 °C. Dashed curve was calculated with equation (2) given in the text. The following parameters were used, $a_1 = 10$ mA/cm², $b_1 = 0.087$ µs^{-1}, $c_1 = 0.500$ µs^{-1}. Experiment 13-D-1. *Insert*: equivalent circuit for squid axon membranes. Z is the passive dielectric impedance, R_s is the series resistance including intra- and extracellular electrolytes, R_L represents the time-independent leakage resistance. From FitzHugh & Cole (1973) with minor changes.

These records show that one of the components of the membrane capacity was charged and discharged with a finite time constant. This raises the question as to whether the finite charging–discharging time was caused by an imperfect capacity, or whether it arose from a distorted membrane potential step (only partial compensation for the effects of the resistance in series with the axolemma was possible during these experiments). As a first approximation the time course of the transients is reproduced by the following expression

$$I = a_1 (\exp(-b_1 t) - \exp(-c_1 t)), \qquad (2)$$

where $a_1 = 10.0$ mA/cm², $b_1 = 0.087$ µs^{-1} and $c_1 = 0.50$ µs^{-1}.

The charge entering this capacitor can be calculated as

$$Q = \int_0^\infty I \mathrm{d}t.$$

For the transients shown in this figure, $Q = 4.515$ nC. Since the displacement in membrane potential (ΔV) was 100 mV,

$$C = Q/\Delta V = 0.045\ \mu\text{F}.$$

The membrane area (estimated from measurements of the diameter in the central part of the fibre) facing the virtual-ground external current electrode plates (Keynes & Rojas 1974) was 0.05 cm², resulting in an estimate of the membrane capacity as 0.90 μF/cm².

From the value of the constant c_1 we estimate the resistance in series with the capacitative element of the membrane as 11.5 Ω cm². One third of this series resistance is generated across the Schwann cell layer, connective tissue and external solution. The remainder originates in the layer of internal solution between the electrode bridge and the membrane (see table 1 of Rojas & Atwater 1968).

Recently, FitzHugh & Cole (1973) have calculated the current transients for a system with constant phase angle capacitance, parallel leakage conductance and series resistance. The equivalent circuit proposed has been drawn in figure 1.

For a constant phase angle capacitance, or constant phase angle impedance, we have

$$Z = |Z|\ (\mathrm{j}\omega)^{-\alpha}, \tag{3}$$

where $\mathrm{j} = (-1)^{\frac{1}{2}}$, $\omega = 2\pi f$. α is related to the phase angle, ϕ, by

$$\phi = \tfrac{1}{2}\alpha\pi.$$

Taylor (1965) measured Z (for f between 10 and 70000 Hz) and could account for the results with $\alpha = 0.85$ (which gives a constant phase angle of $-76.5°$). The difference between the behaviour of a loss-free membrane capacity, where $\alpha = 1$, and a lossy one, where $\alpha = 0.85$ for example, may be important for the analysis of the early behaviour of the nonlinear component of the total membrane capacity. By the method suggested by FitzHugh & Cole (1973) we have estimated α for the transients shown in figure 1 as 0.8.

3. Sodium currents and asymmetrical displacement currents

During most experiments several electrical parameters were measured. The following runs were typical.

(*a*) In fibres internally perfused with caesium fluoride solution and externally bathed in K-free artificial seawater (K-free a.s.w.), using a compensated feed-back control system, sodium currents were measured for various depolarizations from a holding potential of −100 mV.

(*b*) Next, the external K-free a.s.w. was replaced by another a.s.w. containing 107 mM NaCl and 333 mM tris Cl, tris Cl being used in place of NaCl to maintain tonicity and ionic strength. Under these conditions the following records were made: (1) initial time course of the sodium currents for various potential steps from holding potentials ranging from −150 to −50 mV; (2) determination of the rate at which the sodium currents turn off at different times during repolarization.

(*c*) After the series of experiments (*a*) and (*b*) in low sodium seawater, the external solution was replaced by another saline free of sodium and potassium, with the usual concentrations of calcium and magnesium. In most experiments tetrodotoxin (TTX) was added to block the selectivity filter. Under these conditions, ionic currents are severely reduced and the following records could easily be made. (1) Displacement current detected in single sweeps recorded

at high current amplifier gain, for various potential steps from holding potentials ranging from −150 to +50 mV. (2) Signal averager summation of asymmetrical displacement currents for pulses of various sizes and for holding potentials covering the same range. (3) In many experiments we studied the variations of the displacement currents at the end of the pulses as a function of the duration of the pulses.

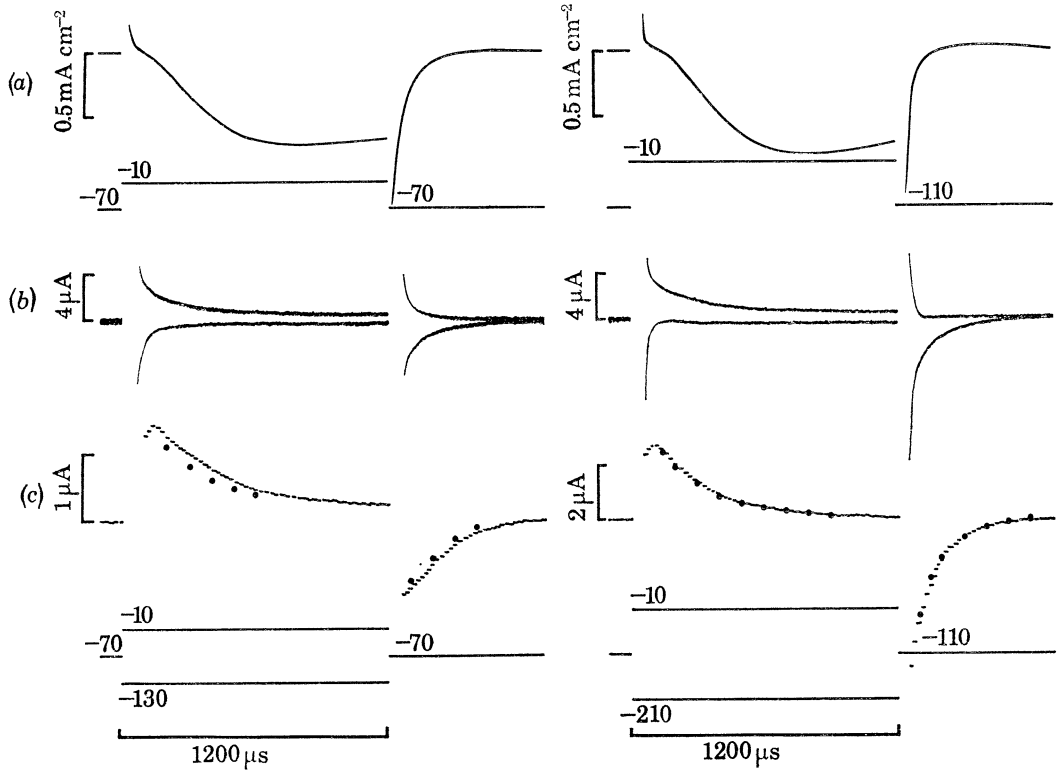

FIGURE 2. Comparison between sodium inward currents and asymmetrical displacement currents. First the fibre was perfused with 300 mM CsF solution and bathed in ¼ Na a.s.w. (107 mM NaCl, 323 mM tris Cl, 10 mM $CaCl_2$, 50 mM $MgCl_2$, pH = 7.3). At this time the records shown in (*a*) were made. The series resistance compensation was set to 4.6 Ω cm². Next, the external low sodium a.s.w. was replaced by a Na- and K-free saline (440 mM tris isethionate, 10 mM calcium chloride, 50 mM magnesium chloride, 300 nM TTX, pH = 7.3) and in this solution the displacement current records shown in (*b*) and (*c*) were made. Traces in (*b*) are single sweep records of displacement currents. Traces in (*c*) are the signal averager records of the sum of 300 pairs of the transients shown in (*b*). The points drawn on top of the signal averager records represent the algebraic sum of the corresponding points in the transients shown in (*b*). For left hand set of records, $V_{hold} = -70$ mV, $\tau_m\ (-10) = 202$ μs at 8 °C. The time constant of the I_{Na} transient during g_{Na} turn-off was 67 μs, so that $\tau_m\ (-70) = 201$ μs. Not taking the first 150 μs into account, the signal averager records were well described by a single exponential with the following time constants: $\tau\ (-10) = 320$ μs, $\tau\ (-70) = 160$ μs. For right hand set of records, $V_{hold} = -110$ mV. Sodium currents could be fitted with $\tau_m\ (-10) = 205$ μs, $\tau_m\ (-110) = 96$ μs. The corresponding signal averager time constants were $\tau\ (-10) = 267$ μs and $\tau\ (-110) = 137$ μs. Experiment 20-D-3. Membrane potentials during and between pulses are indicated below the current traces.

(*d*) Finally, the K-free a.s.w. was introduced again into the chamber and a standard current–voltage curve determined to obtain the final sodium conductance.

Figure 2 illustrates a few typical traces obtained during some of the runs just described. For the set of records shown on the left side of this figure the holding potential was set at −70 mV, and for those on the right at −110 mV. The upper traces (*a*) represent the sodium inward current during and after sudden displacement of the membrane potential from its holding level

to -10 mV, and back to either -70 or -110 mV. From experiments of this kind, in low external sodium and using compensated feed-back, we were able to calculate the time constant for the activation of the sodium conductance during the pulse, and the time constant for turning the sodium conductance off during repolarization, by the procedure of Hodgkin & Huxley (1952). From the voltage dependence of the peak value of the sodium current in the negative resistance region, we could evaluate the steepness of the g_{Na}–V curve.

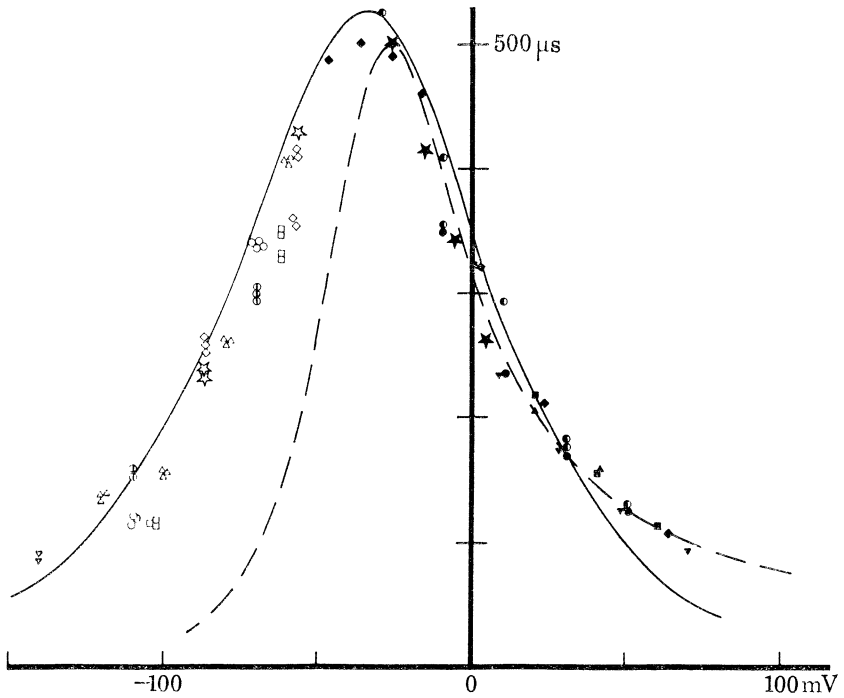

FIGURE 3. Values of τ_m as defined by Hodgkin & Huxley (1952) for the activation of the sodium system, measured in fibres bathed in low Na a.s.w. All experimental points were normalized to a standard temperature of 6.3 °C, assuming a Q_{10} of 3. All fibres were internally perfused with 300 mM CsF plus sucrose, and were bathed externally in $\frac{1}{4}$ Na a.s.w. The smooth curve is drawn according to equation (15*a*) with the parameters obtained from figure 9. The dashed line is the value of τ_m at 6.3 °C calculated from Hodgkin & Huxley (1952), eqns. (20) and (21), resting potential taken as -62 mV. Filled symbols: time constants evaluated from the I_{Na} record during the pulse. Open symbols: from tail records. ●, ○, 20-D-3, 7 °C, compensation set for 4.6 Ω cm²; ■, □, 20-D-1, 7 °C, compensation set for 4.6 Ω cm²; ▲, △, 13-D-1, 8 °C, compensation set for 4.6 Ω cm²; ▼, ▽, 23-N-2, 8.5 °C, compensation set for 4 Ω cm²; ◆, ◇, 21-D-2, 6.2 °C, compensation set for 2.5 Ω cm²; ★, ☆, 21-D-1, 7 °C, compensation set for 4 Ω cm²; ●, ⊕, 18-D-1, 7.5 °C, compensation set for 4.6 Ω cm².

The middle traces (*b*) show the displacement currents remaining when the same pulses are applied after removing external sodium and blocking with tetrodotoxin. Graphical summation of the current transients in figure 2*b* is represented by the dots drawn on top of the sum given by the signal averager (records in figure 2*c*). A brief inspection of these records indicates that the two sums agree rather well, demonstrating that the signal averager does not distort the original signals. A comparison of the current transients after the pulses in figures 2*a*, *b* and *c* indicates that the rate at which the sodium currents decay during g_{Na} turn-off is appreciably greater than the rate of decline of the displacement currents (records in figures 2*b* and *c*). A quantitative comparison is presented later on in figure 10.

Figure 3 represents values of the time constant τ_m calculated for the sodium conductance turn-on and turn-off, and figure 10 the corresponding time constants for the displacement currents, determined in a series of experiments like the one illustrated in figure 2. The temperature varied between 6 and 9 °C and was allowed for by assuming a Q_{10} of 3 (Hodgkin & Huxley 1952). The smooth curve was drawn from equations (15*a*) and (15*b*) given in the text (see also figure 10). The experimental points are well fitted by the curve over the physiological range of membrane potentials. The dashed curve in figure 3 was drawn from the equation given by

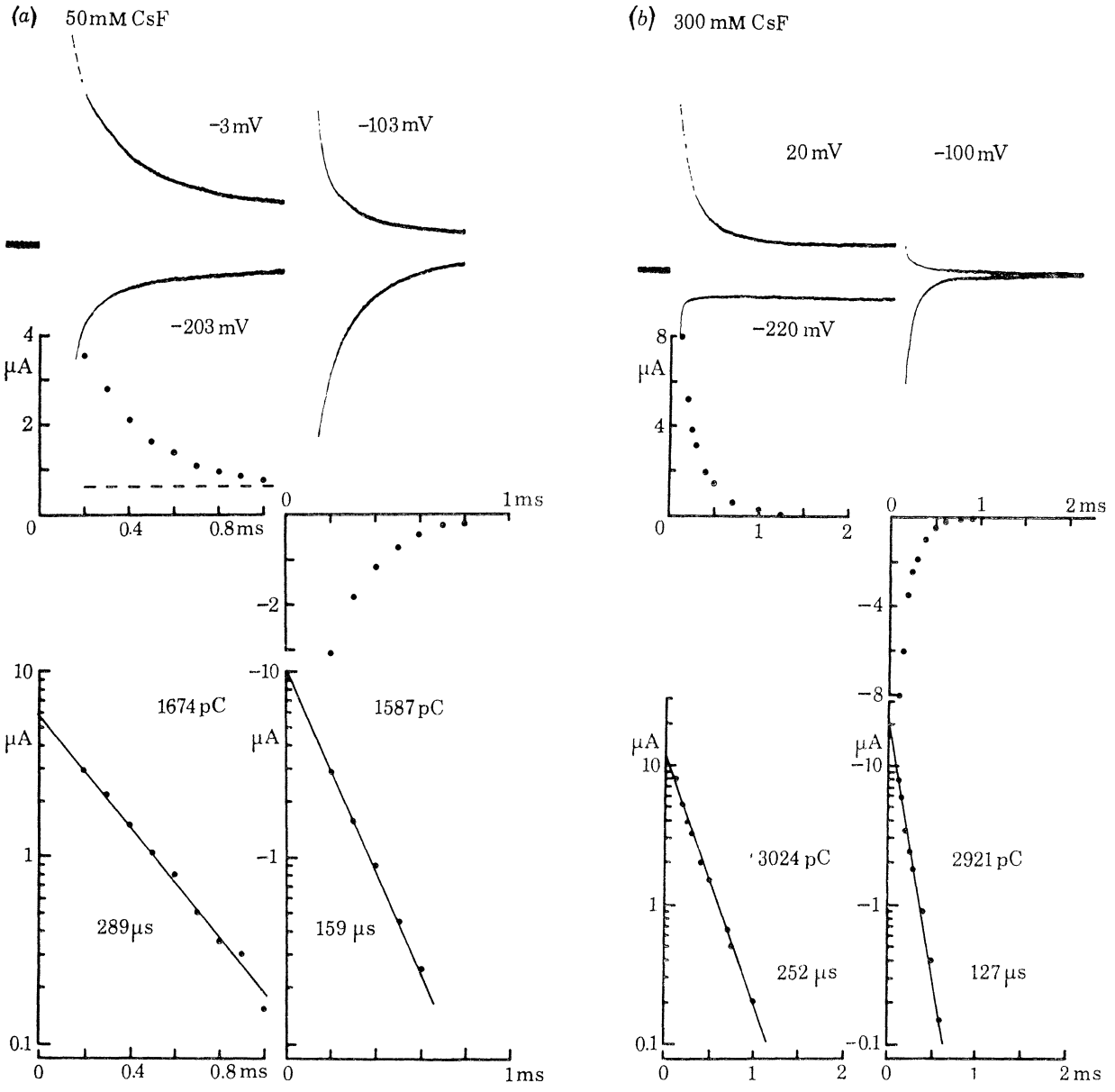

FIGURE 4. Displacement currents in single sweep records.

(*a*) Fibre perfused with a low ionic strength CsF solution (50 mM CsF, 900 mM sucrose, 5 mM tris Cl, pH 7.3) and externally bathed in Na- and K-free saline made with isethionate replacing chloride. Temperature, 6 °C. For this experiment 30-0-1, there was a leakage rectification producing a rectangular outward current in the records obtained with the signal averager.

(*b*) Fibre perfused with 300 mM CsF plus sucrose. For this experiment, 23-N-2, the leakage system did not rectify.

Hodgkin & Huxley (1952) for the relaxation time constant of the first order m-process. For membrane potentials from -60 to -150 mV, which is the range that Hodgkin & Huxley did not examine experimentally, there was a substantial disagreement with their curve, any experimental time constants being greater than those represented by the dashed curve. To be able to compare the distribution of the relaxation time constants for the activation of the sodium conductance and for the asymmetrical displacement currents, the voltage dependence predicted by equations (15a) and (15b) has been shown in both figures 3 and 10.

4. Asymmetrical displacement currents in single-sweep high-gain current records in fibres perfused with 50 and 300 mM CsF

The analysis of the temporal course of the individual asymmetrical displacement current transients is of great importance to resolve the initial time course and to elucidate the question of mechanism. Figure 4 presents two sets of displacement current transients depicted from complete runs in fibres perfused with 50 (figure 4a) or 300 mM CsF (figure 4b). Absolute membrane potentials during and after the pulses have been indicated near the corresponding current transients of figure 4. Beneath these records we present the graphical summation of points taken from the traces shown in the upper part. For the 50 mM CsF case, we assume that the sum did not reach the zero level but that there was some 'leakage rectification' (Keynes & Rojas 1974) amounting to 0.6 μA. Below these graphs, we present semi-logarithmic graphs of the sums using the same time scale. The experimental points are on straight lines. It can be concluded, therefore, that the net asymmetrical charge displacement (represented by the algebraic sum of the individual currents) follows an exponential temporal course. The charge displaced during a pulse of infinite duration (membrane potential step)

$$q\,(V,\,\infty) = \int_0^\infty I_{\mathrm{D}}(V,\,t)\,\mathrm{d}t,$$

equals

$$q\,(V,\,\infty) = I_{\mathrm{D}}\,(V,\,0)\,\tau(V),$$

where $I_{\mathrm{D}}(V,\,0)$ is the extrapolated initial value of the displacement current and $\tau(V)$ is its time constant. These values are indicated in figure 4. It is clear that the charge transferred in one direction during the pulses (1674 and 3024 pC for figures 4a and 4b respectively) is moved back during repolarization (1587 and 2921 pC).

A formal description of the question of charge balance involves the evaluation of the following integrals

$$\int_0^\infty I_{\mathrm{D}}(V,\,t)\mathrm{d}t = \int_0^T I_{\mathrm{D}}(V_p,\,t)\mathrm{d}t + \int_T^\infty I_{\mathrm{D}}(V_{\mathrm{hold}},\,t)\mathrm{d}t, \qquad (4)$$

where the potential is taken to a value of V_p at $t = 0$, and returned to V_{hold} at $t = T$. A quantitative analysis revealed that the charge displaced during the pulses was of exactly the same size as that displaced after the pulses, but the direction of its movement was opposite. This was true regardless of the duration (from 0.2 to 3.0 ms) and the size (from 10 to 160 mV) of the pulses used and, although the range covered was not as ample as desirable, of the temperature of the solution bathing the fibre.

Figure 5 represents a quantitative analysis of the integrations carried out using some of

the results from an early group of experiments with fibres perfused with 55 mM CsF (see table 3 in Keynes & Rojas 1974), and some more recent results working with fibres perfused with 300 mM CsF. The vertical axis represents the charge displacement during the pulses,

$$\int_0^T I_D(V_p, t)\, dt,$$

and horizontal axis represents the charge displacement after the pulses,

$$-\int_T^\infty I_D(V_{hold}, t)dt.$$

The numbers in parentheses in figure 5 indicate the duration of the pulses, T, and the measured time constant for the sodium inactivation, τ_h, respectively. Inactivation of the charge displacement of the kind reported by Armstrong might be expected to decrease the value of

$$-\int_T^\infty I_D(V_{hold}, t)\, dt,$$

and the points in figure 5 corresponding to the longer pulses should then be shifted towards the vertical axis. However, the results presented in this figure demonstrate that the principle of charge balance holds good for all the pulse durations tested.

That the principle of charge balance remains true for pulses with a duration equal to or even greater than the measured time constant for the sodium inactivation carries important

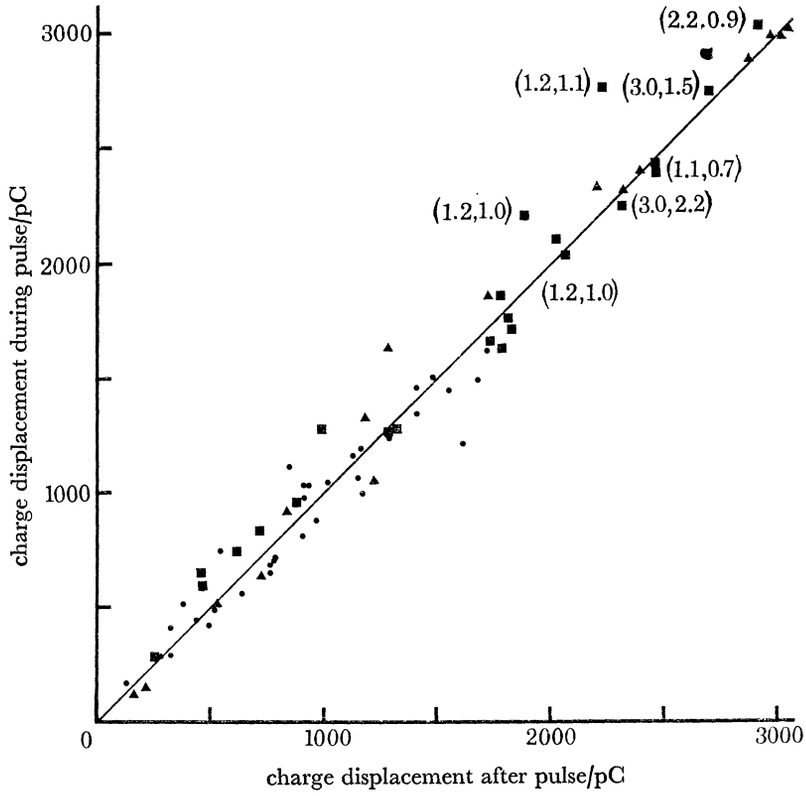

FIGURE 5. The balance of charge displacement. The least-squares regression line had a slope of 0.98 ± 0.05 (s.e.). Numbers in parenthesis indicate the duration of the pulse and τ_h in ms, calculated from the corresponding I_{Na} record. •, Experiments from table 3 in Keynes & Rojas (1974) fibres perfused with 50 mM CsF; ■, experiments from another series, perfusing with 50 mM CsF, but using longer pulses; ▲, experiments on fibres perfused with 300 mM CsF.

PHILOSOPHICAL TRANSACTIONS OF THE ROYAL SOCIETY B BIOLOGICAL SCIENCES

implications for the question of possible inactivation of displacement current discussed by Armstrong (see p. 449). To resolve possible discrepancies between our results, which suggest that the displacement currents do not inactivate with a time constant comparable to τ_h, and Armstrong's observations, it would be desirable to test the validity of the principle of charge balance in experiments of the kind reported by Armstrong, i.e. in low external sodium and without TTX.

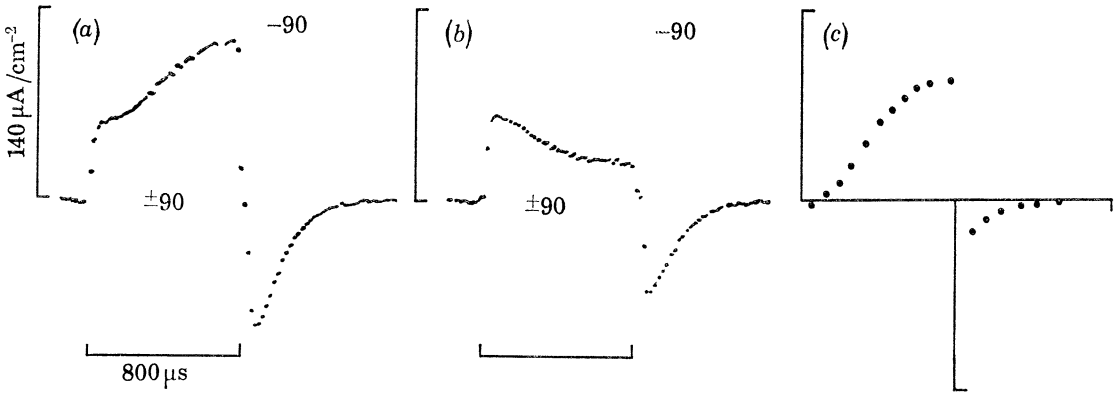

FIGURE 6. Separation of ionic currents from displacement currents. Fibre perfused with 50 mM CsF plus sucrose and bathed in (*a*) Na and K free, tris Cl saline, (*b*) same solution plus 300 nM TTX. $V_{hold} = -90$ mV. (*c*) was obtained by subtracting (*b*) from (*a*). There is a clear TTX-sensitive component in the outward currents shown in (*a*) that is carried by Cs^+. During repolarization there is another TTX-sensitive component that is presumably carried by Ca^{2+} ions permeating the Na channels. Experiment 9-J-1.

We have made some initial comparisons and found certain differences between our records without TTX and the records presented by Armstrong. Thus, figure 6 illustrates two records from the signal averager obtained with a fibre perfused with CsF and bathed in a Na- and K-free saline (record *a*) and in a Na- and K-free saline plus TTX (record *b*). Record *c* represents the graphical difference, *a*–*b*. It is clear from this last graph that TTX has blocked an outward component of ionic current which, since the main cation inside the fibre is Cs^+, is carried by caesium with a permeability ratio $P_{Na}/P_{Cs} = 29$. This early outward current component was not apparent in Armstrong's records. Also shown in this last figure is a small 'tail' of inward current which too is blocked by TTX. These results are in agreement with observations that the early outward current carried by cations other than sodium is blocked by TTX (Rojas & Atwater 1967) and that calcium ions can permeate the membrane through the sodium channels (Baker, Hodgkin & Ridgway 1971). Therefore a drawback of experiments of the kind reported by Armstrong, carried out in low external sodium and without TTX, resides in the fact that in the absence of TTX, membrane current transients are apt to be contaminated by ionic flows in both directions, inwards and outwards, and it is not clear how to separate them from the displacement currents. We think that the evidence provided in figure 5 strongly indicates that in the presence of TTX we are measuring displacement currents. Consequently, a comparison of the current integrals during and after the pulses, in experiments with and without TTX, should enable one to separate ionic currents from displacement currents.

5. Interpretation of the results

Let us summarize the basic properties of the displacement currents (see Keynes & Rojas 1974).

(*a*) The temporal course of the displacement currents produced by sudden displacement of the membrane potential is exponential, and is characterized by a single time constant as evidenced by the experiments presented in figure 4. Furthermore, if we subtract from the current transient obtained with a membrane potential step the faster current transient through the linear component of the membrane capacity, which was described in §2, the difference is a displacement current with an exponential fall-off. This is illustrated in figure 7. The individual current transients which were used to calculate the displacement current are also shown.

(*b*) The time constant is a function of the temperature and of the absolute level of the potential to which the membrane is taken during the step. The normalized data on time constants presented in figure 10 (see also Figure 20 in Keynes & Rojas 1974) is well fitted by the asymmetrical $\tau(V)$ function from equations (12*a*) and (12*b*). Values of $\tau(V)$ from various experiments carried out at different temperatures were reduced to a temperature of 6.3 °C by adopting the temperature coefficient given by equation (18) in the text.

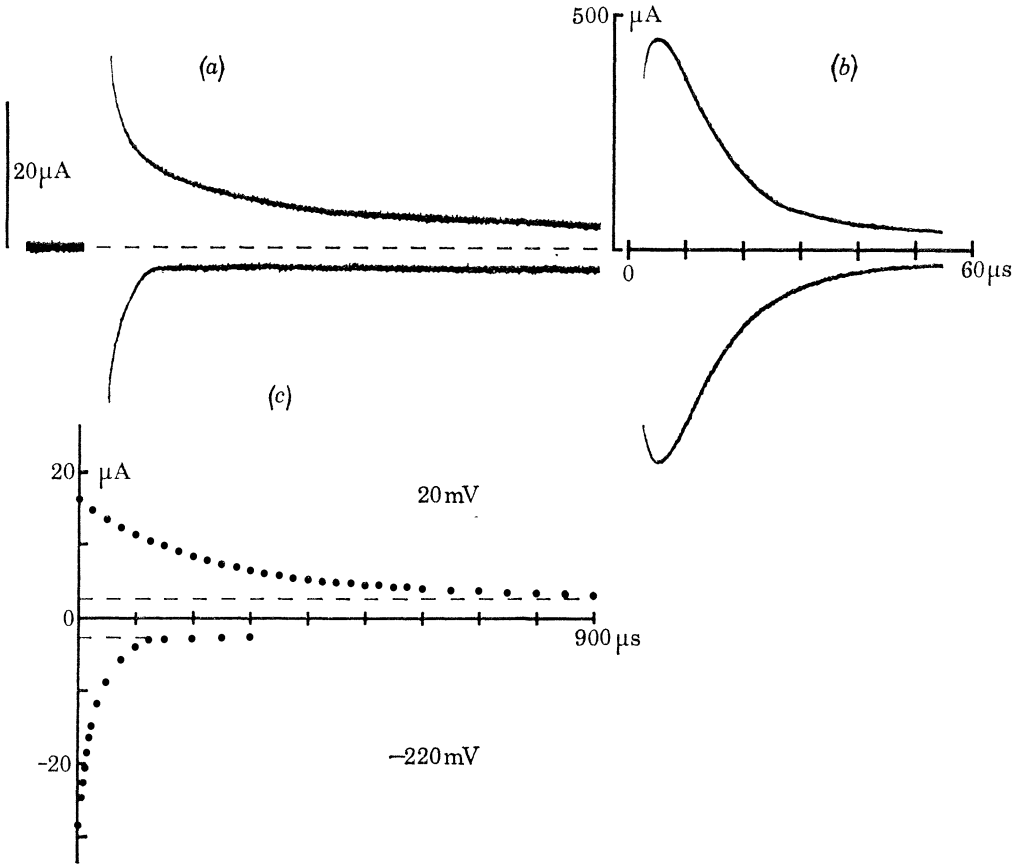

Figure 7. Initial time course of displacement currents recorded in single sweeps. Fibre internally perfused with 300 mM CsF plus sucrose. (*a*) The initial time course of the membrane currents recorded after a sudden change of membrane potential from −100 to either +20 or −220 mV. (*b*) The component of the current flowing through the membrane capacity discussed in §2. (*c*) The difference between the transients shown in (*a*) and (*b*) after appropriate scaling of (*b*). Semi-logarithmic plots of the points shown in (*c*) were single exponentials with time constants of 32 μs for the inward current transient and 231 μs for the outward transient.

(*c*) The charge transferred during a given time T by a rectangular pulse to an absolute membrane potential V_p is

$$q(V_p, T) = \int_0^T I_D(V_p, t)\, dt. \tag{5a}$$

Provided the initial conditions are maintained (same absolute membrane potential before the step change) for a series of steps (or pulses of infinite duration) there is a limiting or saturation value defined as

$$\lim_{V_p \to \infty} q(V_p, \infty) = \lim_{V_p \to \infty} \int_0^\infty I_D(V_p, t)\, dt. \tag{5b}$$

The electric field across the low dielectric region of the membrane changes with the potential V across the membrane roughly as

$$2 \times 10^6 V \text{ V/cm}.$$

In practice, with pulses greater than 200 mV one might reach a field strength which would destroy the membrane dielectric. Therefore, this limiting or saturation value of $q(V, t)$ is that corresponding to a potential beyond which any further displacement would not increase appreciably the value of the integral in (5*b*). On the other hand, experimental records last a finite time only and, therefore, $t = \infty$ in equation (5*b*) indicates that either the integration has to be carried out until the value of the integral does not increase appreciably, or that the integral is evaluated as the product $I_D(V_p, 0)\, \tau(V_p)$.

(*d*) The maximum charge available for displacement during a step change in potential is calculated as

$$Q_{max} = \lim_{V_p \to \infty} q(V_p, \infty) + \left(- \lim_{V_p \to -\infty} q(V_p, \infty) \right) \tag{5c}$$

(outward currents are considered as positive and inward currents as negative).

(*e*) There is a resting or holding membrane potential, V_0, from which two potential steps of equal size but opposite direction taking the membrane potential to V_1 and V_2 respectively, would produce displacement currents such that the sum of their integrals is equal to zero. The limiting charge displaced from this potential is equal to

$$\lim_{V_p \to \infty} q(V_p, \infty) = - \lim_{V_p \to -\infty} q(V_p, \infty) = \tfrac{1}{2} Q_{max}.$$

Having summarized the properties of the initial components of the displacement current and having generated a few formal statements about these properties we next present a model which can be used to determine to what extent it is possible to simplify matters, and still reproduce these general properties of the early asymmetrical displacement currents.

6. Energy considerations

(*a*) *Steady state conditions*

Displacement currents represent either the reorientation of dipoles or a redistribution of charges induced by a sudden change in the intensity of the electric field across the membrane. It is likely, however, that in the course of the reorientation, energy barriers are encountered, for otherwise the time constant with which the charges would reorient themselves under the influence of the field would be considerably smaller (Glasstone, Laidler & Eyring 1941); this point will be taken up again in §6*d*. We propose that in the process of reorientation the dipoles have to 'diffuse' over a single energy barrier.

PHILOSOPHICAL TRANSACTIONS OF THE ROYAL SOCIETY B BIOLOGICAL SCIENCES

Figure 8 represents a single energy barrier profile. Initially the dipoles are distributed among the energy troughs ϵ_1 and ϵ_2. Let us consider that there are N_1 dipoles at the energy level ϵ_1, and N_2 dipoles in the position characterized by the energy level ϵ_2.

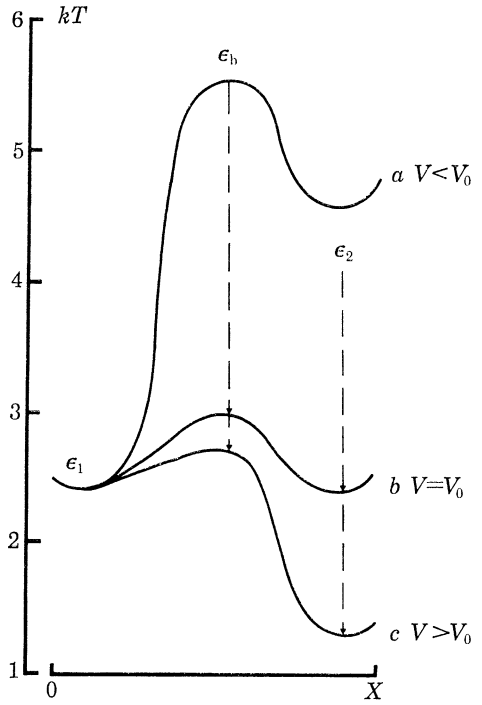

FIGURE 8. Postulated energy profiles before and during step changes in potential. Ordinate: energy level in meV ($1\,kT = 24.2$ meV). Abscissa: reaction coordinate or distance through the membrane. (*a*) postulated single energy barrier profile at $V_{\text{hold}} = -60$ mV before the application of a membrane potential step. (*b*) Energy profile immediately after a sudden change in membrane potential from -60 mV to the transition potential V_0. (*c*) Energy profile immediately after a sudden change in membrane potential from -60 to $+50$ mV.

Assuming that the equilibrium distribution of the dipoles between the two energy states is governed by Boltzmann's law we obtain

$$N_2/N_1 = \exp\{(\epsilon_1 - \epsilon_2)/kT\}. \tag{6}$$

Equating

$$N_1 + N_2 = \frac{L}{aF} Q_{\max}, \tag{7}$$

where a is the effective valence of the dipoles in e.s.u., F is the Faraday constant and L is the Avogadro constant. Combining equations (5*c*) and (7),

$$N_1 = \frac{L}{aF}\{\lim_{V_p \to \infty} q(V_p, \infty) - q(V_p, \infty)\}, \tag{8a}$$

$$N_2 = \frac{L}{aF}\{-\lim_{V_p \to -\infty} q(V_p, \infty) + q(V_p, \infty)\}, \tag{8b}$$

the ratio N_2/N_1 equals

$$\frac{N_2}{N_1} = \frac{-\lim_{V_p \to -\infty} q(V_p, \infty) + q(V_p, \infty)}{\lim_{V_p \to \infty} q(V_p, \infty) - q(V_p, \infty)}, \tag{9}$$

where the right side of equation (9) can be evaluated from records of displacement currents.

Experimentally, $\lim_{V_p \to -\infty} q(V_p, \infty)$ tends to zero if the holding potential V_{hold} is set near -100 mV. In this case equation (9) may be simplified and the following equation used instead

$$\frac{N_2}{N_1} = \frac{q(V_p, \infty)}{Q_{\max} - q(V_p, \infty)}. \tag{10a}$$

It is possible, then, to test equation (6) and to determine the function $\Delta\epsilon$ required to fit the experimental data. Thus

$$\Delta\epsilon = \epsilon_1 - \epsilon_2 = kT \ln \frac{q(V_p, \infty)}{Q_{\max} - q(V_p, \infty)}. \tag{10b}$$

Figure 9*a* represents a graph of the right side of equation (10*b*) as a function of absolute membrane potential. The vertical bars on each experimental point were calculated as the total derivative of the function $kT \ln (q(V_p, \infty)/Q_{\max} - q(V_p, \infty))$ assuming that the error in the value of $q(V_p, \infty)/Q_{\max}$ was about 5 %. Writing

$$\epsilon_1 - \epsilon_2 = aV_0 - aV, \tag{10c}$$

the least squares regression line through the experimental points provided estimates of the

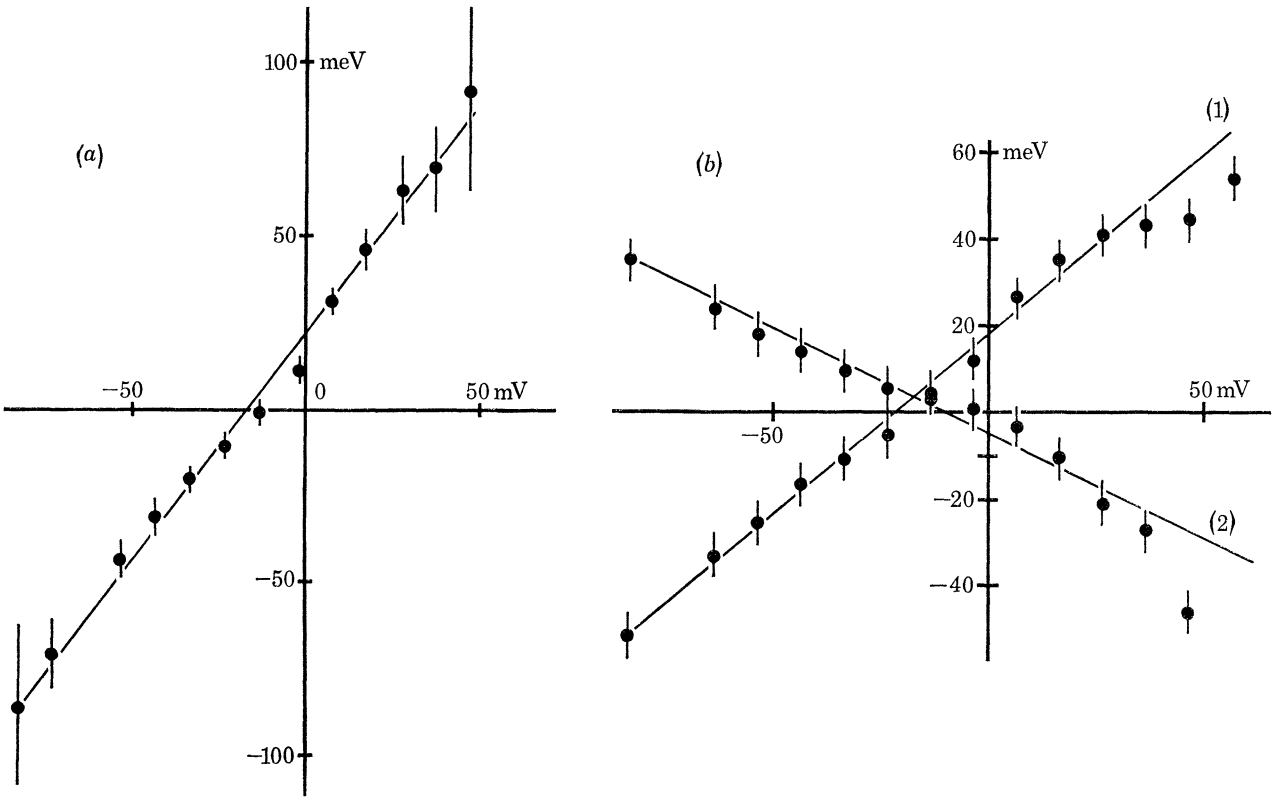

FIGURE 9. (*a*) Evaluation of the energy difference $\epsilon_1 - \epsilon_2$. Vertical bars drawn on each experimental point represent the total derivative of the function $kT \ln \{q/(Q_{\max} - q)\}$ for a maximum error in the determination of $q/Q_{\max}$ smaller than 5 %. The straight line represents the least squares fitting of the points. $V_0 = -17$ mV for this experiment, and $a = -1.3$ e.s.u. The charge displaced during the pulses was estimated from single sweep current transients recorded at high gain. $Q_{\max}$ was reached at an absolute membrane potential of about +50 mV and was equal to 31 nC/cm². Experiment 30-0-1. Fibre internally perfused with 50 mM CsF plus 900 mM sucrose and bathed in a Na, K-free saline made with isethionate in place of chloride.

(*b*) Evaluation of the energy differences $\epsilon_1 - \epsilon_b$ (1) and $\epsilon_2 - \epsilon_b$ (2). Experimental points were calculated as described in the text. Straight lines represent (1) $kT \ln \alpha_0 + (\epsilon_1 - \epsilon_b)$ and (2) $kT \ln \beta_0 + (\epsilon_2 - \epsilon_b)$. Vertical bars show an estimate of the error.

parameters a and V_0 of -1.3 electric charges and -17 mV, respectively. The intercept on the energy axis may be called the apparent ϵ_1, and the intercept on the potential axis, V_0, may be called the apparent transition potential. The values of V_0 and ϵ_1 depend on the experimental conditions and the absolute value of ϵ_1 cannot be determined. Lowering the ionic strength of the internal solution, for example, unshields surface charges inside the membrane (Chandler, Hodgkin & Meves 1965; Rojas & Atwater 1968), which is equivalent to adding to the energy level ϵ_1 an electrostatic energy equal to the product

$$\psi_0 \sigma_0,$$

where ψ_0 is the surface potential and σ_0 is the surface charge density. In view of this last consideration it is possible to interpret the observation that $V_0 \neq 0$ and, therefore $\epsilon_1 \neq 0$, in terms of an asymmetry in the surface potentials (Tsien & Noble 1969). If there were no difference in surface potentials, then the straight line in figure 9*a* should intercept the potential axis at the origin.

Two important conclusions may be drawn from this analysis: (1) the equilibrium distribution of orientation of certain membrane dipoles is consistent with Boltzmann's distribution law and (2) the energy difference between the two allowed states of the possible configurations is a linear function of the transmembrane potential in the range -100 to $+50$ mV.

Using the parameters obtained in figure 9*a* we can calculate the fraction of charges which underwent the transition from state to state and compare it with the quantity $q(V, \infty)/Q_{\max}$ measured experimentally as in figure 19 of Keynes & Rojas (1974).

Having presented evidence that shows that the steady state distribution of charges is governed by Boltzmann's law we now turn to an analysis of the time course of the rearrangement of charges induced by a potential step.

(*b*) *Transition between two types of energy configuration*

Let us consider again the energy diagrams shown in figure 8. If the holding potential before the step is set at -60 mV (curve *a* in figure 8) the energy difference $\Delta\epsilon$ is nearly -50 meV; the dipoles are arranged in such a way that the fraction in either energy configuration is calculated from Boltzmann's law. During the potential step to $+50$ mV, a rearrangement takes place which continues in time until a new equilibrium distribution is achieved. The energy diagram for the new equilibrium distribution is represented by figure 8*c*, for which the energy difference $\Delta\epsilon$ is calculated as $+25$ meV.

The rearrangement of dipoles under the influence of the electric field in the membrane involves some sort of diffusion process. With the evidence at hand it is not possible to determine whether translational diffusion of charges or rotary diffusion of dipoles is involved.

The evidence presented in §5 of this paper strongly suggests that the rearrangement of charges is a first order process. The differential equation describing the transition from position 1 (characterized by the energy level ϵ_1) to position 2 (characterized by the energy level ϵ_2) is therefore equation (1), where k represents the fraction of the total number of charges that underwent the transition.

Assuming that the rearrangement of charges takes place over a single energy barrier, it can be shown that the rate constants are exponential functions of the energy difference between the level from which the charge is being displaced and the level corresponding to the top of the energy barrier (Glasstone *et al* 1941). The problem of rotary diffusion of dipoles with a

PHILOSOPHICAL TRANSACTIONS OF THE ROYAL SOCIETY B BIOLOGICAL SCIENCES

potential barrier located somewhere between the positions characterizing the two states has not been discussed before, and will be presented elsewhere in a more complete analysis of the model (Rojas, in preparation). If one limits oneself to translational diffusion in one dimension, a number of solutions, which are based upon the general results of the theory of Brownian motion, are available (Chandrasekhar 1943). Thus, assuming that the charges move in a potential field without any mutual interference and that the size of the potential barrier is large compared to the energy of thermal motion (24 meV), the probability, per unit time, that particles originally in the potential level ϵ_1 escape to the other state characterized by ϵ_2, over the energy barrier ϵ_b, is equal to

$$P_{1\to 2} = \frac{B}{\xi} \exp\left\{\frac{\epsilon_1 - \epsilon_b}{kT}\right\}, \tag{11}$$

where ξ is the dynamical frictional coefficient and B is a constant.

It should be emphasized here that the rate constant for diffusion from state 1 to state 2 depends on the energy difference $\epsilon_1 - \epsilon_b$, which is the energy barrier for the transition. For the transition in the opposite direction the rate constant depends on the energy difference $\epsilon_2 - \epsilon_b$. In our previous paper these differences were considered identical and equal to $\frac{1}{2}(\epsilon_1 - \epsilon_2)$ (Keynes & Rojas 1974). It follows from equation (11) that the rate constants α and β may be written as

$$\alpha = \alpha_0 \exp\{(\epsilon_1 - \epsilon_b)/kT\}, \tag{12a}$$

$$\beta = \beta_0 \exp\{(\epsilon_2 - \epsilon_b)/kT\}. \tag{12b}$$

The fraction of the total number of charges which are in state 2 at any time is $p = N_2/(N_1 + N_2)$, where p is a function of the absolute membrane potential and time, i.e. $p(V, t)$. To integrate equation (1) with $k = p(V, t)$, we have the following boundary conditions:

$$\text{initial value} = p(V_{\text{hold}}, 0)$$

$$\text{steady state value} = p(V_p, \infty).$$

The solution for equation (1) is then

$$p(V_p, t) = [p(V_{\text{hold}}, 0) - p(V_p, \infty)] \exp(-t/\tau(V_p)) + p(V_p, \infty), \tag{13a}$$

where

$$\tau = \frac{1}{\alpha + \beta}. \tag{13b}$$

Values of $\tau(V_p)$ were collected from different experiments, reduced to a temperature of 6.3 °C using the temperature coefficient given by equation (18), and plotted in the manner shown in figure 10.

(c) *Relation between equilibrium and kinetic properties*

We have described the kinetics of the rearrangement of charges produced by a sudden displacement of the membrane potential. When the equilibrium distribution is reached, then by definition the probability per unit time that particles originally at potential level 1 diffuse to the other state over the potential barrier is equal to the probability that the particles at the potential level 2 diffuse in the opposite direction. From equation (1) we obtain

$$\frac{\alpha}{\beta} = \frac{p}{1-p}. \tag{14a}$$

From equations (12*a*) and (12*b*) this ratio is also equal to

$$\frac{\alpha}{\beta} = \frac{\alpha_0}{\beta_0} \exp\left(\frac{\epsilon_1 - \epsilon_2}{kT}\right). \tag{14b}$$

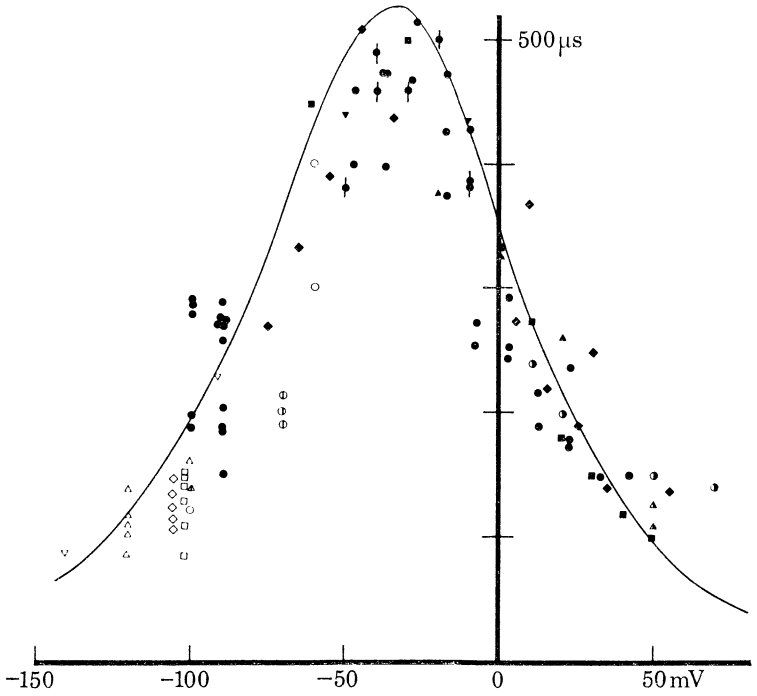

FIGURE 10. Voltage dependence of the relaxation time constant of the displacement current.
●, Time constant values taken from Table 3 in Keynes & Rojas (1974) for fibres internally perfused with 55 mM CsF plus sucrose. Values of potentials for these experiments were shifted 18 mV in a negative direction to take account of the effect of the low ionic strength internal solution.
◆, Data from a more recent group of experiments with 50 mM CsF plus sucrose as internal solution.
■, □, etc., Time constants measured in fibres perfused with 300 mM CsF plus sucrose. Filled symbols, time constants measured during the pulses; open symbols, time constants measured after the pulses at various holding potentials. Data from the group of experiments in which τ_m was measured in low external sodium, as presented in figure 3; the same symbols have been used for this figure. The continuous line was drawn according to equations (12*a*) and (12*b*) with $\alpha_0 = \beta_0 = 0.85$ and $(\epsilon_1 - \epsilon_b) = 24.2 + 0.726$ V and $(\epsilon_2 - \epsilon_b) = -(14.52 + 0.581$ V).

Equation (6), which was derived earlier from the Boltzmann expression, and which has been shown to be applicable to the equilibrium distribution of the charged particles, is now seen to follow also from equations (14*a*) and (14*b*). In equations (13*b*) and (14*a*) we have two expressions for α and β in terms of measured quantities, and can therefore evaluate the rate constants at any given potential. From (12*a*) and (12*b*) it follows that

$$\ln \alpha = \ln \alpha_0 + \frac{\epsilon_1 - \epsilon_b}{kT},$$

$$\ln \beta = \ln \beta_0 + \frac{\epsilon_1 - \epsilon_b}{kT}.$$

In figure 9*b*, $kT \ln \alpha$ and $kT \ln \beta$ are plotted against potential. The values are seen to fall reasonably well on straight lines, whence it may be concluded that the energy differences governing the rate constants are to a first approximation linearly dependent on the membrane potential.

(*d*) *Voltage dependence of the relaxation time constant*

From equations (12*a*), (12*b*) and (13*b*) the relaxation time constant is a function of potential given by

$$\tau(V) = \frac{1}{\alpha + \beta} = \frac{1}{\alpha_0 \exp(\epsilon_1 - \epsilon_b)/kT + \beta_0 \exp(\epsilon_2 - \epsilon_b)/kT}. \qquad (15a)$$

When $V = V_0$, the mid-potential of the steady state distribution curve, then from (10*c*), $\epsilon_1 = \epsilon_2$, and the maximum value of the time constant is seen to be given by

$$\tau(V_0) = \frac{1}{\alpha_0 + \beta_0} \exp(\epsilon_b - \epsilon_1)/kT. \tag{15b}$$

We have shown that the relaxation time constant has a rather large temperature coefficient (Keynes & Rojas 1974). This could arise either from the temperature dependence of the energy barrier ϵ_b, or be introduced in the coefficients α_0 and β_0. The latter seems the more likely in view of the fact that equation (11) contains a dynamical frictional coefficient ξ as a multiplying factor, and this coefficient certainly depends on temperature. Thus, for rotary diffusion under the influence of a moderate electric field of spherical protein molecules free from mutual interactions, the relaxation time constant is given by

$$\tau = \xi/kT \tag{16}$$

(Tandford 1961), where ξ is again the dynamic frictional coefficient. For spherical particles,

$$\xi = 8\pi\eta R^3, \tag{17}$$

where η is the viscosity of the medium and R is the radius of the particles.

If the movement of the dipoles were confined to the low dielectric region of a membrane whose thickness was 4 nm, rotary diffusion of spherical dipoles with a radius close to 2 nm would take place in a medium of a viscosity of 200 mPa s (Mu-ming & Cone 1974) with a time constant of about 3 μs. This value is about 100 times smaller than the measured time constants, and from equations (16) and (17) either the viscosity must be increased by two orders of magnitude, or the radius of the protein must be increased to such an extent that it would no longer fit within the dimensions of the low dielectric region of the membrane. In this connexion it may be noted that decreasing the temperature from 20 to 10 °C is known to increase the viscosity of some oils by a factor of three, and the relaxation time constant might therefore be altered to a similar extent. In line with this explanation, α_0 and β_0 can be expressed in terms of an empirical relation making

$$\alpha_0, \beta_0 \propto \exp\{2(t - 6.3)/kT\}, \tag{18}$$

which reproduces fairly well the temperature dependence of $\tau(V)$ measured experimentally (Keynes & Rojas 1974). The data presented in figures 3 and 10 has been normalized with the help of equation (18).

From the least squares regression lines fitted to the experimental points in figure 9*b* we obtain (in meV)

$$kT \ln \alpha_0 + (\epsilon_1 - \epsilon_b) = 18 + 0.82\ V$$

and

$$kT \ln \beta_0 + (\epsilon_2 - \epsilon_b) = -4.5 - 0.38\ V.$$

The fitting of the experimental points to equation (15*a*) is, as may be seen in figure 10, fairly good over the normal physiological range of membrane potentials, that is from −70 to +40 mV. For potentials outside these limits, the equation predicts that the relaxation time constants should decrease monotonically. Our experiments suggest that even for very large depolarizing pulses taking the potential beyond +100 mV, the time constant is never less than 80 μs. It therefore seems that the energy diagram presented in figure 8 needs to be modified to give rise to definite saturation values for the rate constants.

PHILOSOPHICAL TRANSACTIONS OF THE ROYAL SOCIETY B BIOLOGICAL SCIENCES

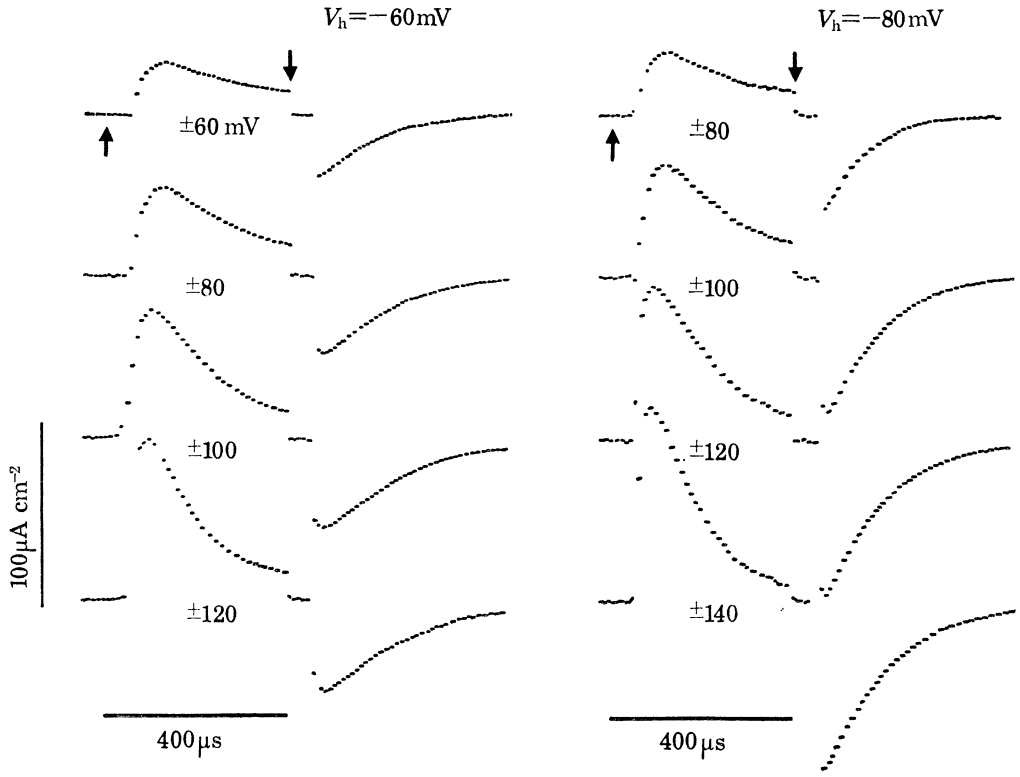

FIGURE 11. Effect of holding potential on the initial time course of net displacement current records. Experiment 13-D-1. Fibre internally perfused with 300 mM CsF plus sucrose. Temperature 7.8 °C. Size of the pulses applied is indicated near each record. Duration of blanking pulses 50 μs.

7. RECONSTRUCTION OF ASYMMETRICAL CURRENT TRANSIENTS

The equation describing the kinetics of the transition can be used to obtain a general expression for the asymmetrical displacement current induced by a membrane potential step from the holding potential, V_{hold}, to a potential V_p that will lie in the depolarizing direction during the test pulse, and in the hyperpolarizing direction during the control pulse, when it will be written as $V_{p'}$. From equation (13*a*) the rate at which the particles are transferred from state 1 to state 2 is

$$\frac{\mathrm{d}p}{\mathrm{d}t} = \frac{1}{\tau(V_p)}\{p(V_p, \infty) - p(V_{\text{hold}}, 0)\} \exp\left(-\frac{t}{\tau(V_p)}\right). \tag{19}$$

Now the displacement current is given by

$$I_{\text{D}}(V, t) = Q_{\max}\, \mathrm{d}p/\mathrm{d}t,$$

so that the result of adding the displacement currents for the test and control pulses will be to give

$$I_{\text{D}}(\text{summed}) = \frac{Q_{\max}}{\tau(V_p)}\{p(V_p, \infty) - p(V_{\text{hold}}, 0)\} \exp\left(-\frac{t}{\tau(V_p)}\right) + \frac{Q_{\max}}{\tau(V_{p'})}\{p(V_{p'}, \infty) - p(V_{\text{hold}}, 0)\} \exp\left(-\frac{t}{\tau(V_{p'})}\right) \tag{20}$$

(cf. Keynes & Rojas 1974, equation (15)).

We have illustrated displacement currents associated with single hyperpolarizing or depolarizing pulses in figures 2, 4 and 7. In these records the current transients through the linear component of the membrane capacity were not subtracted. We have also shown in figures 2*c*, 6*b* and 11 some examples of the summed records obtained with the signal averager. It will be noted that in every case the decline of the current from the initial peak follows a time course very close to a single exponential. Although equation (20) predicts that the net (summed) current obtained with the signal averager should fall off with a time course involving two different time constants, when the holding potential was not less than -100 mV, the control pulse time constant $\tau(V_{p'})$ was always less than 100 μs and $p(V_{\text{hold}}, 0)$ was always small, so that the second term in the equation contributed relatively little after the first 200 μs. When, however, the holding potential was lowered towards the transition potential V_0, the second term in equation (20) became more important, giving rise to a delay in the arrival of the displacement current at its peak. The effect of variation in the holding potential on the time course of the net displacement current is illustrated in figure 11.

8. Effect of holding potential on the direction of the displacement currents

It will be obvious from equation (20) that a reversal of the direction of the net displacement current is to be expected in the neighbourhood of the transition potential V_0. If the curve relating $\tau(V)$ to potential were symmetrical about V_0, then for V_{hold} more negative than V_0 the net current would be outwards, while for V_{hold} less negative than V_0 it would be inwards. For $V_{\text{hold}} = V_0$ the net current would be zero at all times. An asymmetry in the $\tau(V)$ curve would slightly displace the holding potential at which the initial net displacement current, $I_{\text{D, 0}}$, passed through zero, although the total net charge displacement,

$$\int_0^T I_{\text{D}}(V_p, t)\,\mathrm{d}t + \int_0^T I_{\text{D}}(V_{p'}, t)\,\mathrm{d}t,$$

would still be zero at $V_{\text{hold}} = V_0$.

The experiments illustrated in figures 12 and 13 were designed to examine the effect of varying the holding potential on the direction of the displacement current. First, in figure 12, we show single sweep records taken at holding potentials on either side of V_0, which in this case was about -40 mV. With $V_{\text{hold}} = -100$ mV as in *a*, the net displacement current was obviously outwards, while with $V_{\text{hold}} = 0$ mV as in *d*, it was just as obviously inwards. At intermediate holding potentials the difference between the records for the depolarizing and hyperpolarizing pulses was less marked, but it can nevertheless be seen that the net current was still outwards with $V_{\text{hold}} = -60$ mV as in *b*, and that at -20 mV as in *c* it had reversed. Beneath the current traces photographed on the oscilloscope, we have drawn the time course of the displacement currents calculated from the two terms in equation (20), after subtracting the capacity transient by the procedure used in figure 7. The lessening of the difference in mobile charge displacement between the positive and negative pulses as V_{hold} approaches -40 mV is clearly visible.

On several occasions we set out to test the validity of the principle of charge balance at the beginning and end of the pulse, after altering the holding potential. In experiments like that of figure 12 where the external chloride had been replaced by isethionate, the results were entirely satisfactory, but when this precaution was not taken, as in the experiments illustrated

in figure 13, anionic leakage currents were apt to confuse the issue. In cases like figure 13*b*, application of a positive pulse when the holding potential was already +50 mV gave rise to a leakage current that did not appear as a rectangular pedestal, but altered progressively with time, making it hard to measure objectively either the total charge displacement or the gating current time constant. This difficulty did not, however, affect the size or time course of the

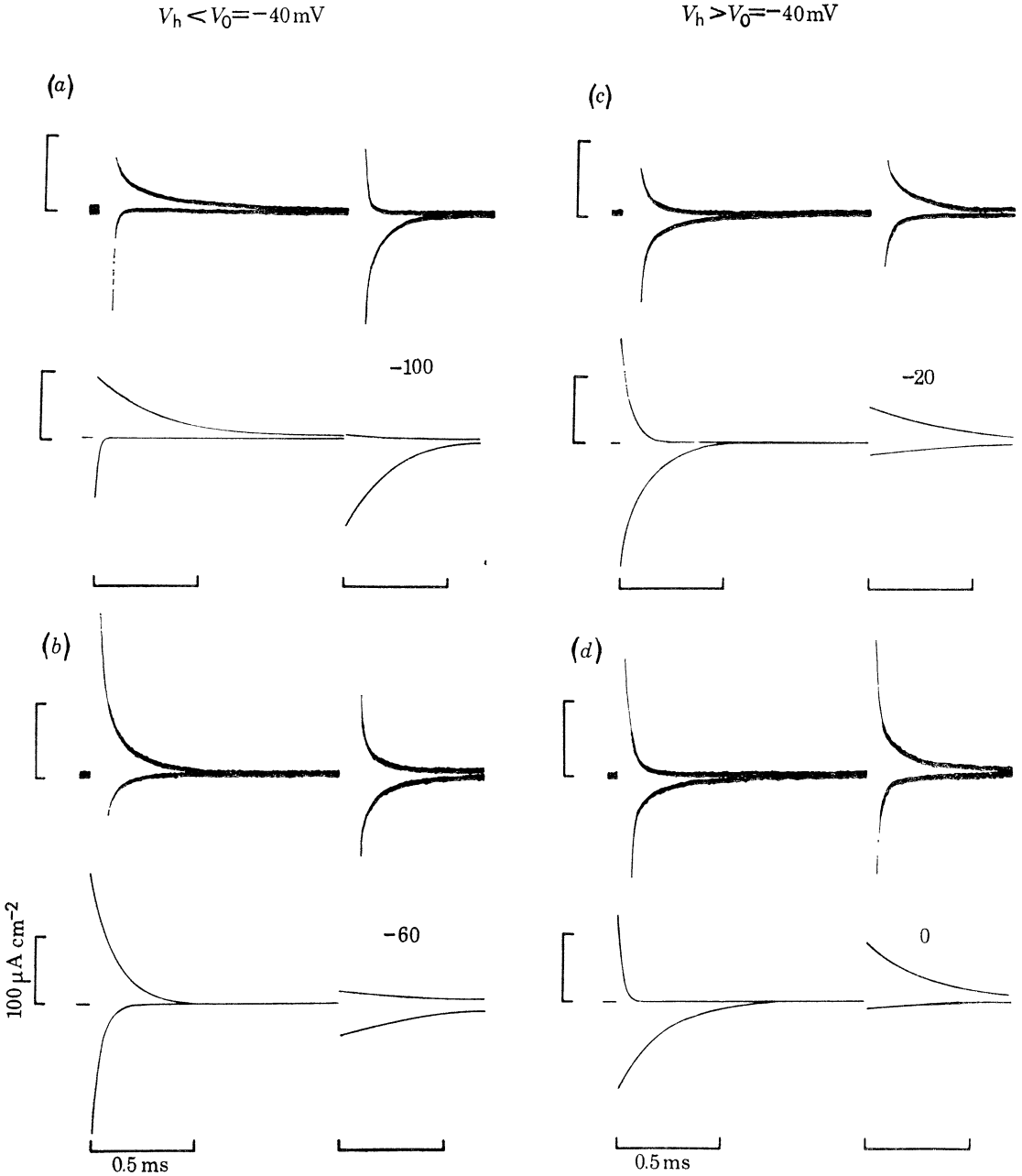

FIGURE 12. Analysis of the effects of holding potential upon the displacement current recorded in single sweeps. Experiment 20-D-1. Fibre internally perfused with 300 mM CsF plus sucrose, and bathed in Na- and K-free saline plus 300 nM TTX made with isethionate in place of chloride. Temperature 6.4 °C. Four sets of current transients are shown: (*a*) and (*b*) were recorded with V_{hold} at values more negative than the measured transition potential $V_0 = -40$ mV. (*c*) and (*d*) were made for V_{hold} values more positive than V_0. The holding potential is indicated next to each group of records. Below each current transient the calculated time course of I_D is shown. These I_D curves were calculated for $Q_{max} = 30$ nC/cm², $V_0 = -40$ mV and $a = -1.3$ e.s.u.

asymmetrical charge displacement on returning to the holding potential at the end of the pulse. The experiment of figure 13*b* was one of four in which the membrane potential was held at +50 mV for not less than 3 min before recording the displacement current. We feel that it provides convincing evidence that at least under the conditions of our experiments at Plymouth, the gating current is *not* inactivated by prolonged depolarization of the membrane, as has been reported by Armstrong & Bezanilla (1974).

Figure 13*a* shows the results of an experiment designed to compare the values of V_0 obtained on the one hand by reducing the holding potential until the displacement currents were

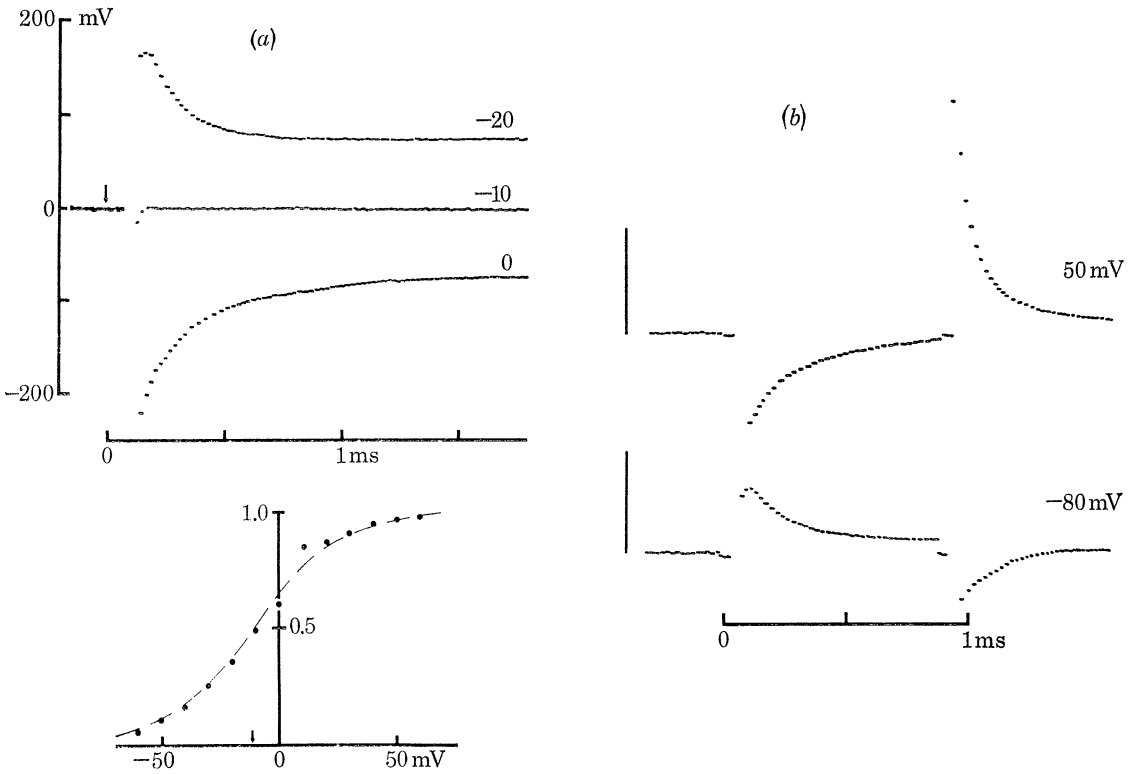

FIGURE 13. (*a*) Two methods of determining the transition potential. Above: fibre internally perfused with 50 mM CsF plus sucrose, and bathed in 110 mM $CaCl_2$, 280 mM tris Cl, 50 mM $MgCl_2$ at pH 7.3, plus 300 nM TTX. For each tracing the membrane potential was held at the level indicated to the right. The membrane was subjected alternately to equal pulses of ±150 mV. Blanking that lasted for 50 μs was applied at the beginning and end of the pulses. Below: the net displacement current measured from a set of records obtained with $V_{hold} = -100$ mV. Dashed curve was calculated from $p = \alpha/(\alpha+\beta)$, where α and β are given by equations (12*a*, *b*). Apparent $V_0 = -11$ mV. Experiment 21-N-2.

(*b*) Net displacement current recorded with V_{hold} set at +50 mV and −80 mV. Experiment 23-0-1. Fibre perfused with 50 mM CsF plus sucrose, and bathed in 430 mM tris Cl, 10 mM $CaCl_2$, 50 $MgCl_2$ at pH 7.4. Temperature 7 °C. For the run with $V_{hold} = +50$ mV the fibre was kept at this potential for 185 s. Immediately after this run, V_{hold} was returned to −80 mV and the lower record was made. Vertical calibrations equal 100 mV.

inverted, and on the other by determining the midpoint of the steady state charge distribution curve with V_{hold} maintained at −100 mV. Trouble from instability of the leakage current was in this instance minimized by raising the external calcium concentration to 110 mM. In the records above it is seen that the net displacement current was outwardly directed with $V_{hold} = -20$ mV, and was inwards with $V_{hold} = 0$ mV; at a holding potential of −10 mV, the record was practically flat. From the graph below, the alternative method of measuring

the transition potential gave a value of -11 mV. Since the axon was both perfused with a low ionic strength solution and exposed to high calcium, it was not surprising to find that V_0 was shifted some distance in a positive direction from the value expected for an intact axon in normal calcium.

Although in this case the two methods of measuring V_0 were in good agreement, there were others in which the potential at which the signals were inverted was appreciably more negative than the midpoint of the steady state distribution curve. Especially when V_{hold} was maintained at a positive value for any length of time, the inversion potential could be as much as 30 mV more negative than the midpoint of the steady state curve. In the experiments like figure 13*b*, for example, the inversion potential averaged -45 mV while the midpoint of the steady state curve lay at -25 mV. It is not yet clear why these discrepancies sometimes arise, and it can only be suggested that they may somehow result from the superimposition on the mechanism controlling the rapid movements of the gating particles of a much slower process affecting the electric field seen by the particles.

9. Conclusions

From their analysis of the kinetics and steady state properties of the ionic conductance system, Hodgkin & Huxley (1952) proposed that the conductance of the sodium channels varied as the cube of the time and voltage-dependent parameter m. Now, let us assume that in series with the sodium selectivity filter described by Hille (1970, 1972) there are a number of charged gating particles. If sodium ions can pass through the filter and the gate only when *all* the particles controlling a given channel have undergone the transition from state 1 (closed) to state 2 (open), it is possible to estimate the number of gating particles per channel by applying Boltzmann's law both to the curve for peak sodium conductance and to that for the steady state distribution of the particles. The least change in membrane potential to produce an e-fold change in sodium conductance is 6 mV, while the corresponding figure for an e-fold change in charge displacement is 19 mV (Keynes & Rojas 1974). The ratio $19/6 = 3.1$ should yield the effective cooperation number for activation of the sodium channels, independently of any factor related to the efficiency with which the membrane potential displaces individual mobile charges. It is rather satisfactory thus to be able to confirm Hodgkin & Huxley's (1952) choice of a cube law for activation of sodium conductance with an argument based on entirely different premises.

We have presented evidence supporting the notion that the activation of each sodium channel involved the displacement of three charged particles from a blocking position to an open position. This immediately raises the question whether the subsequent inactivation of the sodium conductance might not likewise depend on a somewhat slower displacement of another type of charged particle from an open position to a blocking position. If this were the case, the observed displacement current would represent the sum of the m and h gating currents, and should have a component displaying h kinetics. From equation (20) it has been seen that the displacement current is proportional both to the forward rate constant and to the total charge displacement. The latter might well be much the same for m and h, since the steepness of Hodgkin & Huxley's h_∞ curve suggests that the h particles might carry just about enough extra charge to compensate for their smaller number. The value of τ_h, on the other hand, will probably be nearly ten times that of τ_m in the range of membrane potentials covered in most of our experiments. Hence the h component of the gating current will not be much more than a tenth of the size

of the *m* component, and might be difficult to disentangle from the pedestal of leakage current. While we have as yet been unable to identify an *h* component in any of our records, we cannot be certain that it does not exist.

If there are three particles per channel each with an effective valency of 1.3, and if Q_{max} is taken from Table 5 of Keynes & Rojas (1974) as 1882 $e/\mu m^2$, we may estimate the density of sodium channels in the squid giant axon as 483 μm^{-2}. This agrees in order of magnitude with determinations of the number of high-affinity tetrodotoxin or saxitoxin binding sites reported at this Meeting, which were based both on the use of tritiated tetrodotoxin (Levinson & Meves 1975) and on studies of the rate of blocking of sodium conductance (Keynes, Rojas & Taylor 1973; Keynes, Bezanilla, Rojas & Taylor 1975). Taking the peak sodium conductance of the membrane as 120 mS/cm², the conductance of a single sodium channel would therefore be about 2.5 pS.

We are indebted to Dr B. Rudy for assistance with some of our experiments, and to Sir Andrew Huxley, F.R.S., for helpful comments. Part of the work was done during tenure of an M.R.C. Senior Visiting Fellowship by E.R.

References (Rojas & Keynes)

Armstrong C. M. & Benzanilla, F. 1974 Charge movement associated with the opening and closing of the activation gates of the Na channels. *J. gen. Physiol.* **63**, 533–552.

Baker, P. F., Hodgkin, A. L. & Ridgway, E. B. 1971 Depolarization and calcium entry in squid giant axons. *J. gen. Physiol.* **218**, 709–755.

Chandler, W. K., Hodgkin, A. L. & Meves, H. 1965 The effect of changing the internal solution on sodium inactivation and related phenomena in giant axons. *J. Physiol., Lond.* **180**, 821–836.

Chandrasekhar, S. 1943 Stochastic problems in Physics and Astronomy. *Rev. Mod. Phys.* **15**, 1–342.

FitzHugh, R. & Cole, K. S. 1973 Voltage and current clamp transients with membrane dielectric loss. *Biophys. J.* **13**, 1125–1140.

Glasstone, S., Laidler, K. J. & Eyring, H. 1941 In *The theory of rate processes*. New York: London: McGraw-Hill.

Hille, B. 1970 Ionic channels in nerve membranes. *Prog. Biophys. & mol. Biol.* **21**, 1–32.

Hille, B. 1972 The permeability of the sodium channel to metal cations in myelinated nerve. *J. gen. Physiol.* **59**, 637–658.

Hodgkin, A. L. & Huxley, A. F. 1952 A quantitative description of membrane current and its application to conduction and excitation in nerve. *J. Physiol., Lond.* **117**, 500–544.

Keynes, R. D., Bezanilla, F., Rojas, E. & Taylor, R. E. 1975 The rate of action of tetrodotoxin in the squid giant axon. *Phil. Trans. R. Soc. Lond.* B **270**, 365–375. (this volume).

Keynes, R. D. & Rojas, E. 1974 Kinetics and steady-state properties of the charged system controlling sodium conductance in the squid giant axon. *J. Physiol., Lond.* **239**, 393–434.

Keynes, R. D., Rojas, E. & Taylor, R. E. 1973 Saxitoxin, Tetrodotoxin barriers and binding sites in squid giant axons. *J. gen. Physiol.* **61**, 267 (abstract 42).

Levinson, S. R. & Meves, H. 1975 The binding of tritiated tetrodotoxin to squid giant axons. *Phil. Trans. R. Soc. Lond.* B **270**, 349–352 (this volume).

Mu-ming, P. & Cone, R. A. 1974 Lateral diffusion of rhodopsin in the photoreceptor membrane. *Nature, Lond.* **247**, 438–441.

Rojas, E. & Atwater, I. 1967 Effect of tetrodotoxin on the early outward currents in perfused giant axons. *Proc. natn. Acad. Sci. U.S.A.* **57**, 1350–1355.

Rojas, E. & Atwater, I. 1968 An experimental approach to determine membrane charges in squid giant axon. *J. gen. Physiol.* **51**, 131–145s.

Tandford, C. 1961 *Physical chemistry of macromolecules*. New York: John Wiley.

Tsien, R. W. & Noble, D. 1969 A transition state theory approach to the kinetics of conductance changes in excitable membranes. *J. Membrane Biol.* **1**, 248–273.

Taylor, R. E. 1965 Impedance of the squid axon membrane. *J. cell. comp. Physiol.* **66**, 21–25.

PHILOSOPHICAL TRANSACTIONS OF THE ROYAL SOCIETY B BIOLOGICAL SCIENCES